Supporting Information

Saha et al. 10.1073/pnas.1114854108

SI Materials and Methods

UV Radiation Plates. The UV unit (Bioforce Nanoscience Inc., USA) was used to generate high-intensity UV light, which can excite molecular oxygen to form atomic oxygen and ozone. Compared with the reduced pressure plasma treatment used to manufacture commercial TCPS, UV treatment is a straightforward process that does not require relatively expensive gas handing and vacuum processing equipment. In this study, untreated polystyrene (Corning), polypropylene (Grainger), or Ultra-Low Attachment surfaces containing a neutral hydrophilic hydrogel coating (Corning) were oxidized at a distance of around 4 cm from the UV lamp, and results are reported for exposure times under atmospheric conditions after preheating the UV lamp for 30 min. Chemically heterogeneous surfaces (patterned surfaces) were obtained by a simple masking technique. The custom-made stainless-steel photomask was placed on the surface of the untreated polystyrene dish and treated in the unit as above. Treated surfaces could be stored under ambient room temperature conditions for at least 6 mo.

Cell Culture. Before cell seeding, UV-treated surfaces were coated at room temperature for 15 min with either recombinant human vitronectin (0.2–3 μg/mL in DMEM/F12 base medium; R&D Systems), 20% human serum (vol/vol in DMEM/F12; Sigma), or 20% FBS (lot no. AVC63371, cat no. SH30070.03, vol/vol in DMEM/F12; HyClone). For this coating procedure, serum percentage may need to be optimized from 5–40% depending on the batch of serum. Because we saw identical behavior between recombinant vitronectin and serum for any assay on our engineered substrates, we used serum to reduce the cost of many experiments by 10-fold.

hESC (BG01, WIBR1, and WIBR3) and previously established hiPSC lines were maintained on mitomycin C-inactivated mEF feeder layers in standard medium (1). BG01-Oct4-GFP hESCs were made by introducing an Oct4-GFP-puro construct into hESCs (2). hiPSCs (C1 cell line only) were derived through lentiviral infection of Oct4, Sox2, and Klf4 and cultured on mEFs as described previously (3).

For FACS sorting, hESC or hiPSC lines were cultured in 10 μM ROCK inhibitor (Y-27632; Stemgent) for 12–24 h in standard mEF conditions before sorting. Cells were harvested enzymatically with 1 mg/mL collagenase and then with 0.05% trypsin for 5 min at 37 °C. hiPSCs were immunoassayed using SSEA-4. Cells were collected in media with ROCK inhibitor and sorted on a FACSAria flow cytometer (Becton Dickinson). Cells were subsequently plated on various surfaces in medium supplemented with ROCK inhibitor (4) for the first 8–12 h of culture to reduce initial apoptosis of completely dissociated hESCs. Short-term addition of other small molecules [e.g., blebbestatin (5, 6), thiazovivin (7)] that inhibit apoptosis, enhance motility, or up-regulate E-cadherin could also help single-cell growth. For FBS/human serum/vitronectin-coated UV-treated surfaces, culturing occurred in mTESR1 (Stem Cell Technologies), TeSR2 (Stem Cell Technologies), or AF NutriStem hESC XF (Stemgent) media. Long-term culture on UV-treated surfaces occurred in mTeSR1 media and by passaging at a ratio of 1:3 every 5–7 d using either mechanical passaging and collagenase or accutase (StemPro Accutase; Invitrogen) for single-cell enzymatic passaging. ROCK inhibitor was added during the first 8–12 h for the single-cell enzymatic passaging.

ToF-SIMS. A secondary ion mass spectrometer (ION-TOF; IV) was operated using a Bi_3^+ primary ion source operated at 25 kV and in "bunched mode." A 1-pA primary ion beam was rastered on an area of 100 × 100 μm. Secondary ions were collected from the same area over a 10-s acquisition time. Ion masses were determined using a high-resolution ToF analyzer allowing accurate mass assignment. The typical mass resolution (at m/z = 41) was just over 6,000. Nitrogen-containing ions in the spectra likely arise from incorporation of air in the UV unit. ToF-SIMS images were acquired using random raster in a high-current bunched mode.

Numerical Analysis of Surface Chemistry. Principal component analysis (PCA) and PLS regression were carried out using the Eigenvector PLS_Toolbox 3.5 utilizing the SIMPLS algorithm. For least-squares regression, Excel (Microsoft) was used.

XPS. XPS was carried out on a Kratos Axis Ultra instrument using monochromated Al Kα radiation (1,486.6 eV), a 15-mA emission current, a 10-kV anode potential, and a charge-compensating electron flood. High-resolution core levels were acquired at a pass energy of 20 eV. The takeoff angle of the photoelectron analyzer was 90°.

Image Analysis to Monitor Cell Aggregation. To quantify cell aggregate size after cell seeding, hESCs were passaged at a seeding density of 12,000 onto six-well plates with varying UV-patterned surfaces. After 24 h, cell aggregates were observed using phase-contrast microscopy and images were recorded at a magnification of 4×. To quantify the size of aggregates, image analysis was performed using ImageJ (National Institutes of Health). The images were converted to binary using an automated thresholding function, and colony areas were computed using particle analysis.

Flow Cytometry Analysis. Cells were dissociated using accutase and resuspended in 0.5% paraformaldehyde in PBS. Cells were then analyzed on a FACSCalibur flow cytometer (Becton Dickinson) within 7 d. Histograms were generated in FlowJo (Tree Star, Inc.).

Stem Cell Migration Modeling and Simulation. To understand and predict the effects of micropatterned surfaces on the survival and colony formation of stem cells better, a numerical model was implemented.

Individual stem cells were modeled as circles with a 30-μm diameter seeding randomly on a round 2D surface representing a single micropatterned "spot," with the locations of cells represented as x,y coordinate points. In the absence of neighbors, cells are assumed to move in random motion defined by random unit vectors on the unit circle.

In the presence of neighboring stem cells, single cells appear to migrate preferentially toward others and to form small aggregates (8). This was modeled in the simulation as directed movement toward nearest cells at two-thirds of normal speed under a threshold distance of 110 μm. Cells closer than 30 μm were treated as a colony and allowed to random-walk within 30 μm of each other. This allowed cell aggregates to migrate preferentially toward other single cells and cell aggregates. Cells were assumed to move at 9 μm/h, and simulations were run for 24-h periods at different cell seeding densities and on different-sized micropatterned surfaces.

From the final cell locations on the 2D surface, the number and size of cell colonies were counted using the Statistics Toolbox

in MATLAB (MathWorks). The pairwise distances between all pairs of cells in the simulation were computed using the PDIST function utilizing the Euclidean distance method:

$$d_{ab} = \sqrt{(x_a - x_b)(x_a - x_b)^T}$$

where x_a and x_b represent coordinate x,y pairs defining the final locations of cells a and b.

From the pairwise distance calculations, an agglomerative cluster tree relating individual cells by distance was created using the linkage function in MATLAB. Starting from individual cells, clusters were built up of nearest neighbor cells first, and these clusters were linked in levels based on shortest distance clustering, the minimum distance between elements of each cluster:

$$\min(d_{ab}(a,b) : a \in A,\ b \in B)$$

where a and b represent cells a and b of clusters A and B, respectively.

Colonies were defined as consisting of cells located less than 30 μm from at least one other cell in a cluster. Using the MATLAB function cluster, colonies were constructed from the agglomerative hierarchical cluster tree generated by the linkage function above, setting the cutoff criterion distance as 30 μm.

Immunocytochemistry. As described previously (1), samples were washed with PBS, fixed with 4% (vol/vol) paraformaldehyde solution for 20 min, permeabilized with 1% (vol/vol) Triton X-100 in PBS for 45 min if staining for a nuclear protein (Oct4, Sox2, or Nanog), and then stained overnight with following primary antibodies: GFP (with OG5 cultures), SSEA-4, TRA-1-60 (Millipore), TRA-1-81 (Invitrogen), Nanog, Sox2, and Oct4. Alexa-Fluor secondary antibodies were then added. The nuclei were stained with Hoechst.

Teratoma Assay. hESC or hiPSC aggregates were collected by centrifugation, resuspended in 250 μL of PBS, and injected s.c. in the back of SCID mice (Taconic). Tumors generally developed within 4–8 wk, and animals were killed before tumor size exceeded 1.5 cm in diameter. Teratomas were isolated and fixed in formalin. After sectioning, teratomas were diagnosed on the basis of H&E staining.

Karyotypic Analysis. Chromosomal studies were performed by Cell Line Genetics using standard protocols for high-resolution G-banding.

Lentiviral Infection and hiPSC Derivation. Reprogramming used a loxP-flanked version of the pHAGE-STEMCCA vector (9), which is a Cre-exisable polycistronic vector encoding Oct4, Sox2, Klf4, and cMyc reprogramming factors driven by a constitutive EF1α promoter. Vesicular stomatitis virus G protein (VSVG)-coated lentiviruses were generated in 293 cells as described previously, except human serum replaced FBS and mTeSR1 was used during reprogramming (10). In brief, culture medium was changed 24 h after transfection and virus-containing supernatant was collected 48–72 h after transfection. Viral supernatant was filtered through a 0.45-mm filter. Virus-containing supernatants were pooled for infections and supplemented with an equal volume of fresh culture medium. One million patient-derived human fibroblasts ("237" and "267" samples) were seeded 24 h before transduction in T75 flasks. Four consecutive infections in the presence of 2 μg/mL polybrene were performed over a period of 48 h. Culture medium was changed 12 h after the last infection. Five days after transduction, fibroblasts were passaged with trypsin and replated onto "UV-Pattern." For the first 4 d, cells were cultured in 20% human serum in DMEM-F12 media and then switched to mTeSR1 media. The hiPSC colonies were picked manually on the basis of morphology between 2 and 4 wk and manually maintained and passaged.

Gene Modification and Vector Excision. For gene targeting or Cre-recombinase–mediated vector excision, hESC/hiPSC lines were cultured in ROCK inhibitor 24 h before electroporation. Cells were harvested with accutase, and 1×10^7 cells resuspended in PBS were transfected with the appropriate plasmids by electroporation (250 V, 500 μF, 0.4-cm cuvettes; Gene Pulser Xcell System; Bio-Rad) as described previously (11, 12). For vector excision, 50 μg of pCre-PAC (13) was used. We targeted the promoter of PPP1R12C (the AAVS1 locus) using a gene-trap vector containing a SA-2A-puromycin selection cassette (11). Cells were subsequently plated in medium supplemented with ROCK inhibitor for the first 24 h. Cells were selected with the addition of puromycin (2 μg/mL) 2 d after electroporation for a period of 48 h. Individual colonies were picked 10–14 d after electroporation. Excision of reprogramming transgenes was determined as described previously (12) by Southern blot analysis of EcoR1-digested genomic DNA probed against hKLF4.

Live-Cell Imaging. Cells were cultured for the duration of imaging in CO_2-independent medium (Gibco) supplemented with 10 μM ROCK inhibitor, 10% (vol/vol) FBS (HyClone), 1 mM glutamine (Invitrogen), 1% nonessential amino acids (Invitrogen), 0.1 mM β-mercaptoethanol (Sigma), and 40 ng/mL FGF2 (R&D Systems). Cells were imaged over a period of 20 h using a Deltavision (Applied Precision, Inc.) microscope (objective with a magnification of 4× to 10×) and an HQ2 (Photometrics) camera. Time lap intervals were 10 min.

Statistical Testing. All error bars indicate 95% confidence intervals. P values were calculated using Student t tests for binary comparisons or ANOVA for multiple group comparisons.

1. Mei Y, et al. (2010) Combinatorial development of biomaterials for clonal growth of human pluripotent stem cells. *Nat Mater* 9:768–778.
2. Green JJ, et al. (2008) Nanoparticles for gene transfer to human embryonic stem cell colonies. *Nano Lett* 8:3126–3130.
3. Hockemeyer D, et al. (2008) A drug-inducible system for direct reprogramming of human somatic cells to pluripotency. *Cell Stem Cell* 3:346–353.
4. Watanabe K, et al. (2007) A ROCK inhibitor permits survival of dissociated human embryonic stem cells. *Nat Biotechnol* 25:681–686.
5. Ohgushi M, et al. (2010) Molecular pathway and cell state responsible for dissociation-induced apoptosis in human pluripotent stem cells. *Cell Stem Cell* 7:225–239.
6. Chen G, Hou Z, Gulbranson DR, Thomson JA (2010) Actin-myosin contractility is responsible for the reduced viability of dissociated human embryonic stem cells. *Cell Stem Cell* 7:240–248.
7. Xu Y, et al. (2010) Revealing a core signaling regulatory mechanism for pluripotent stem cell survival and self-renewal by small molecules. *Proc Natl Acad Sci USA* 107: 8129–8134.
8. Li L, et al. (2010) Individual cell movement, asymmetric colony expansion, rho-associated kinase, and E-cadherin impact the clonogenicity of human embryonic stem cells. *Biophys J* 98:2442–2451.
9. Sommer CA, et al. (2009) Induced pluripotent stem cell generation using a single lentiviral stem cell cassette. *Stem Cells* 27:543–549.
10. Brambrink T, et al. (2008) Sequential expression of pluripotency markers during direct reprogramming of mouse somatic cells. *Cell Stem Cell* 2:151–159.
11. Hockemeyer D, et al. (2009) Efficient targeting of expressed and silent genes in human ESCs and iPSCs using zinc-finger nucleases. *Nat Biotechnol* 27:851–857.
12. Soldner F, et al. (2009) Parkinson's disease patient-derived induced pluripotent stem cells free of viral reprogramming factors. *Cell* 136:964–977.
13. Taniguchi M, et al. (1998) Efficient production of Cre-mediated site-directed recombinants through the utilization of the puromycin resistance gene, pac: A transient gene-integration marker for ES cells. *Nucleic Acids Res* 26:679–680.

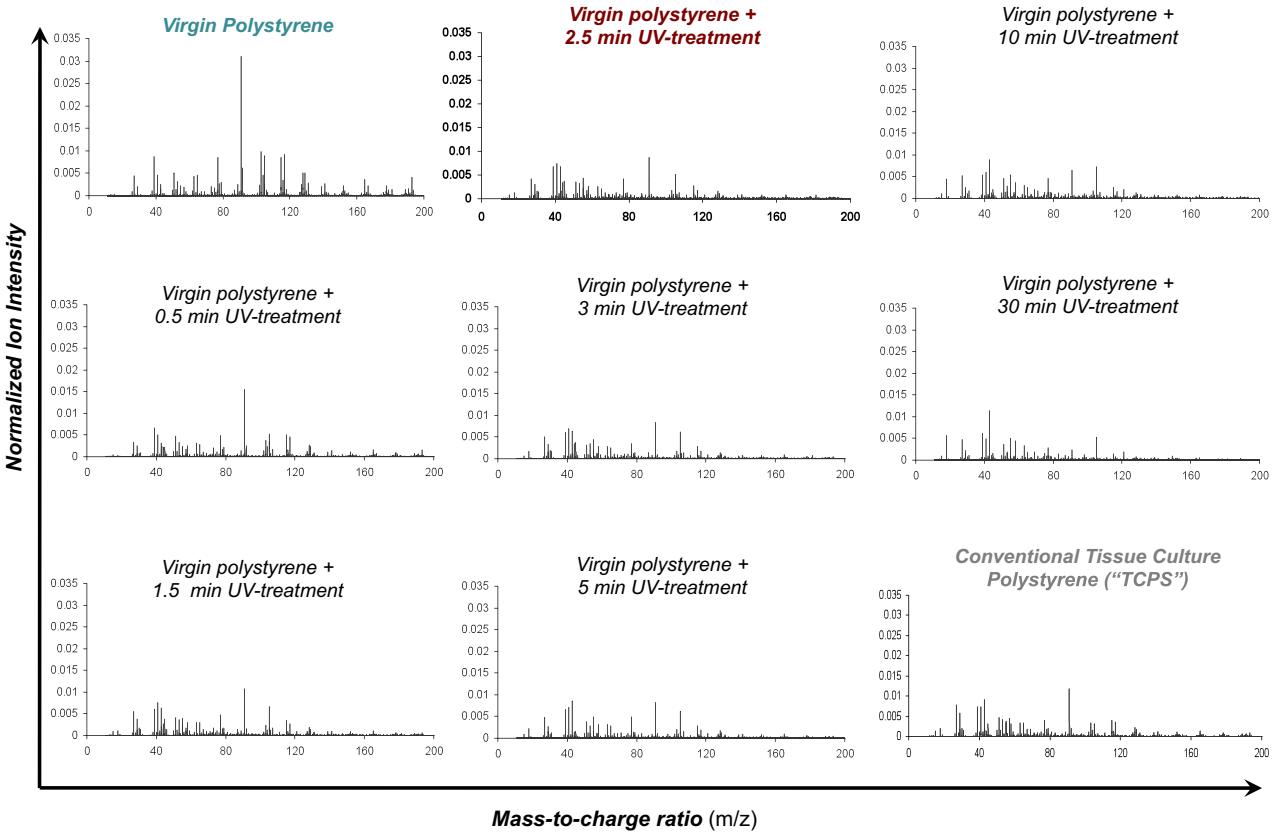

Fig. S1. Controlled modification of substrate surface chemistry. The complete range (*m/z* = 0–200) of spectra from ToF-SIMS of UV-treated substrates. Spectra are shown for virgin polystyrene treated for the indicated times and for conventional TCPS substrates. A detailed analysis of these spectra is provided in Figs. S2 and S3.

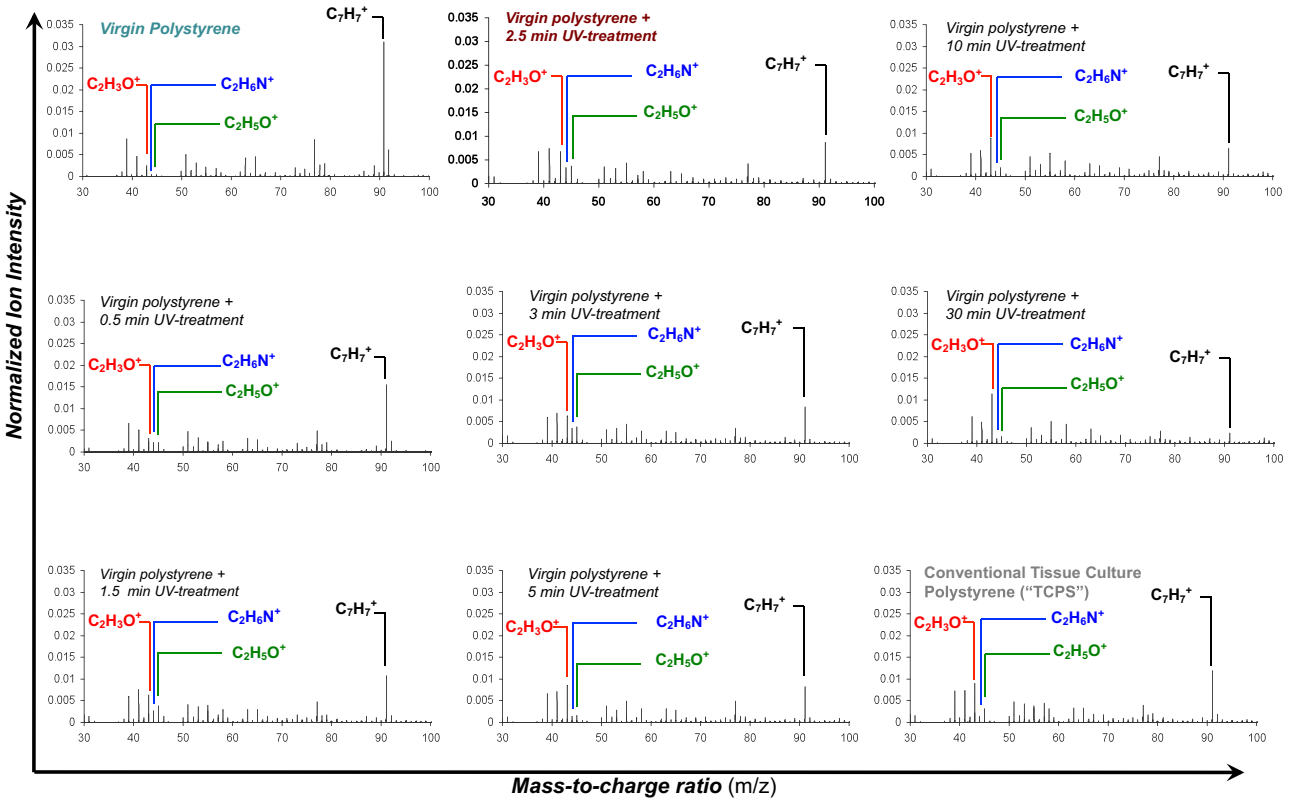

Fig. S2. Example of surface chemistry differences generated by UV treatment. The enlarged section (*m/z* = 30–100) of ToF-SIMS spectra of UV-treated substrates is as shown in Fig. S1. Four specific ions differentially represented on the surfaces are indicated in red, blue, green, and black (ion details are provided in Fig. S3 *A*–*C*). $C_2H_5O^+$ (*m/z* = 45, green line) and $C_2H_6N^+$ (*m/z* = 44, blue line) ions were identified to support hESC colony formation, whereas $C_2H_3O^+$ (*m/z* = 43, red line) ions were identified to inhibit hESC colony formation (Fig. S3C). $C_7H_7^+$ (*m/z* = 91, black line) ions were identified to associate with unmodified virgin polystyrene.

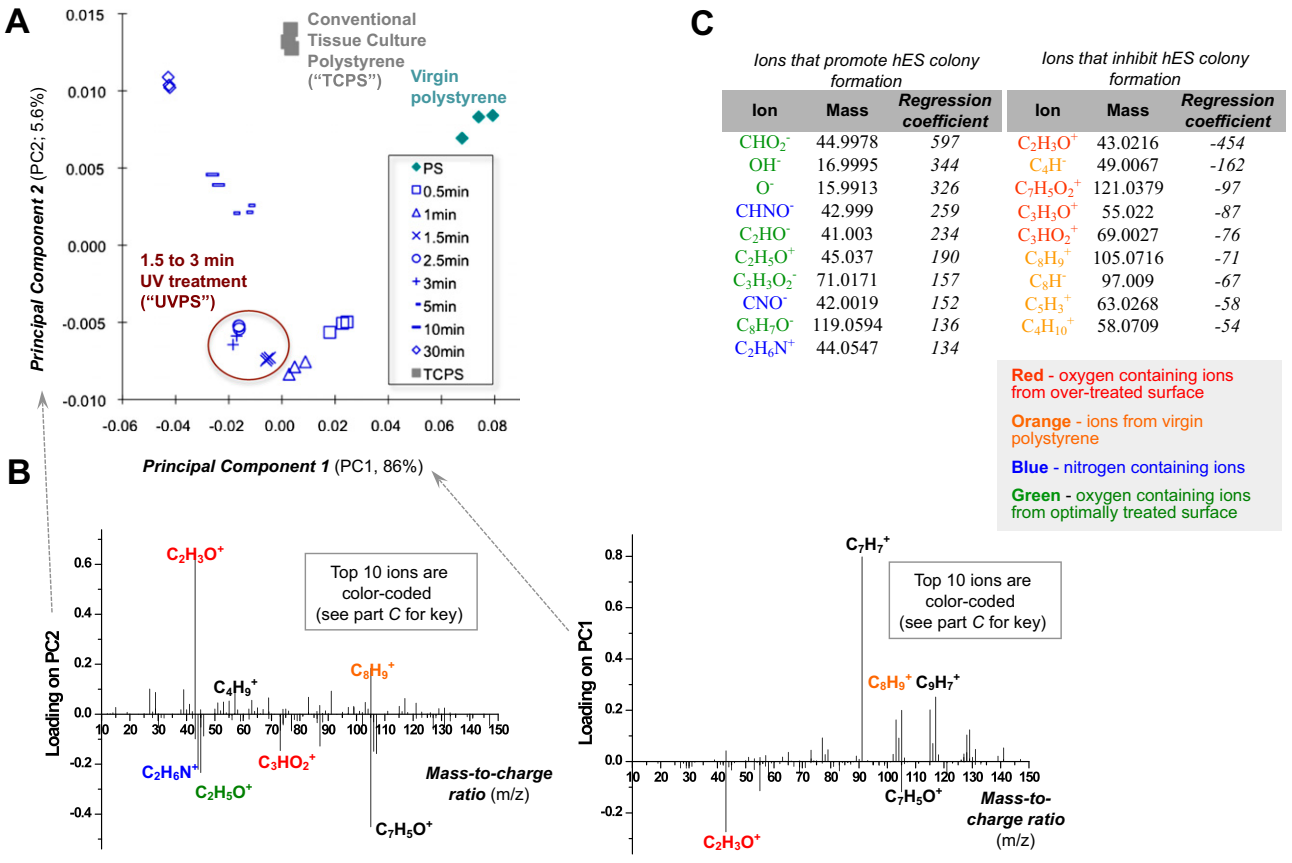

Ion	Mass	Regression coefficient
CHO_2^-	44.9978	*597*
OH^-	16.9995	*344*
O^-	15.9913	*326*
$CHNO^-$	42.999	*259*
C_2HO^-	41.003	*234*
$C_2H_5O^+$	45.037	*190*
$C_3H_3O_2^-$	71.0171	*157*
CNO^-	42.0019	*152*
$C_8H_7O^-$	119.0594	*136*
$C_2H_6N^+$	44.0547	*134*

Ion	Mass	Regression coefficient
$C_2H_3O^+$	43.0216	*-454*
C_4H^-	49.0067	*-162*
$C_7H_5O_2^+$	121.0379	*-97*
$C_3H_3O^+$	55.022	*-87*
$C_3HO_2^+$	69.0027	*-76*
$C_8H_9^+$	105.0716	*-71*
C_8H^-	97.009	*-67*
$C_5H_3^+$	63.0268	*-58*
$C_4H_{10}^+$	58.0709	*-54*

Fig. S3. Surface chemical structures associated with UV treatment. (*A*) Using principal component analysis (PCA) of the ToF-SIMS spectra, samples with similar surface chemistry cluster together in the PCA graph. Each "PC" value in the figure represents a linear combination of peak intensities from the spectra in Fig. S1. Note that the 1.5–3 min of UV treatment (in the red ellipse) optimally supports colony formation (Fig. 1 *C* and *D*). (*B*) Loadings of PC1 and PC2. Loadings reveal the major ions that cause the different values of samples on the PC axis. Ions with positive loading values contribute to larger PC values, and vice versa. For example, virgin polystyrene, with the highest PC1 values, generates the highest intensity of $C_7H_7^+$. (*C*) Using a multivariate PLS model of the ToF-SIMS data, two lists of ions, with the highest or lowest regression coefficients, were identified as supporting (coefficient >0) or inhibiting (coefficient <0) hESC colony formation.

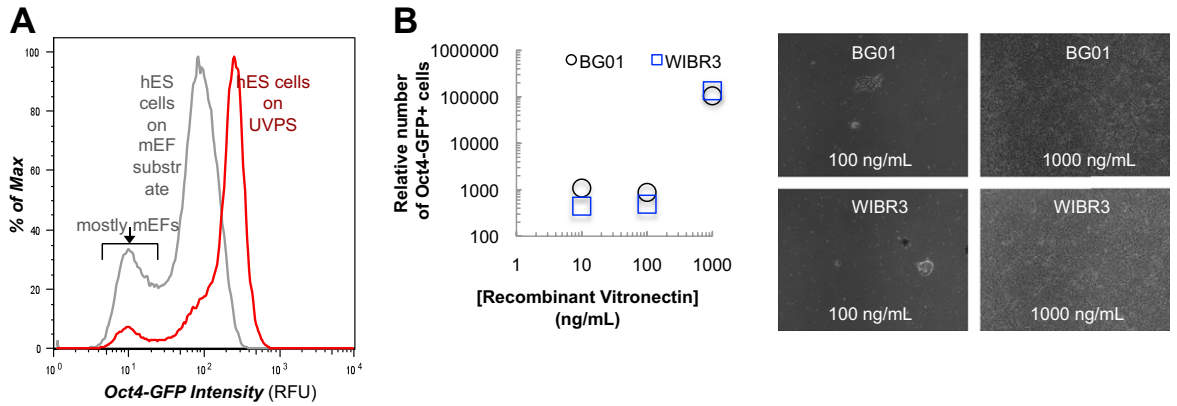

Fig. S4. Chemical optimized substrates allow for undifferentiated cell growth through integrin engagement with vitronectin. (*A*) Flow cytometry histogram of Oct4-GFP levels in UVPS-cultured cells from day 7 (red, treated with optimal 2.5-min UV dose; Figs. S1–S3) and on standard mouse embryonic feeder (mEFs)-containing substrates (gray). The peak near 10^1 relative fluorescence units (RFU) in the gray histogram largely consists of mEFs. UVPS was coated with 20% (vol/vol) FBS in DMEM-F12 base media for 15–30 min at room temperature before cell seeding. Cells were seeded in 10 μM Y-27632 ROCK inhibitor for the first 8–12 h after dissociation. (*B*) Number of pluripotent cells after 5 d for two different cell lines when coated with different concentrations of recombinant vitronectin in PBS(+). One milliliter of the solution per well of a six-well plate (10 cm^2) was used.

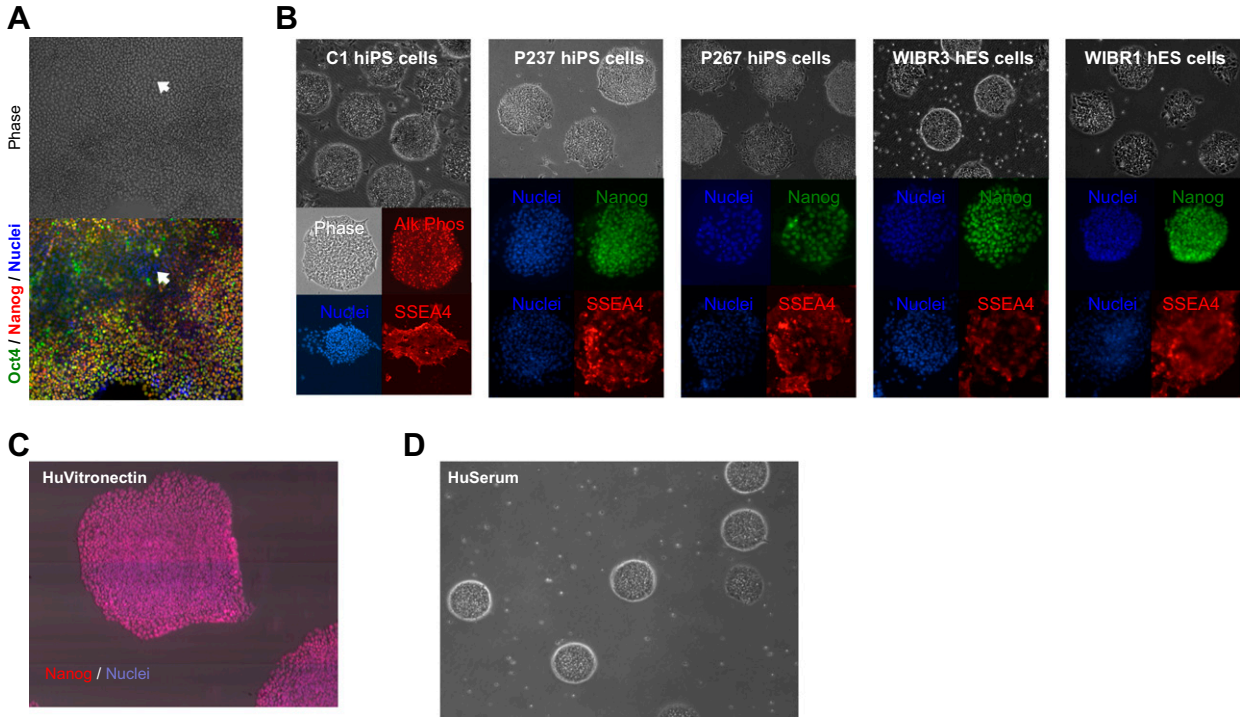

Fig. S5. Modulating cell behavior by patterning culture substrates. (*A*) Large BG01 hESC colony on a UV-treated substrate without any spatial patterning (UVPS). Arrows indicate cells in these large colonies that down-regulate the pluripotency markers Nanog (red) and Oct4 (green). (*B*) (*Upper*) Growth of other human pluripotent cell lines on UV-patterned polystyrene substrates ("UV-Pattern"). (*Lower*) Pluripotency marker staining (colored) after one to three passages is shown for each labeled cell line. Surfaces were coated with 20% (vol/vol) FBS in DMEM-F12 base media for 15–30 min at room temperature before cell seeding. Cells were seeded in 10 μM Y-27632 ROCK inhibitor for the first 8–12 h after dissociation. (*C*) Immunostaining for the pluripotency marker Nanog on BG01 hESCs on UV-Pattern coated with human vitronectin after 7 d of culture. (*D*) Phase-contrast images of BG01 hESCs on UV-Pattern coated with 20% (vol/vol) human serum in DMEM-F12 base media after 7 d of culture. The figure is a composite of multiple panels.

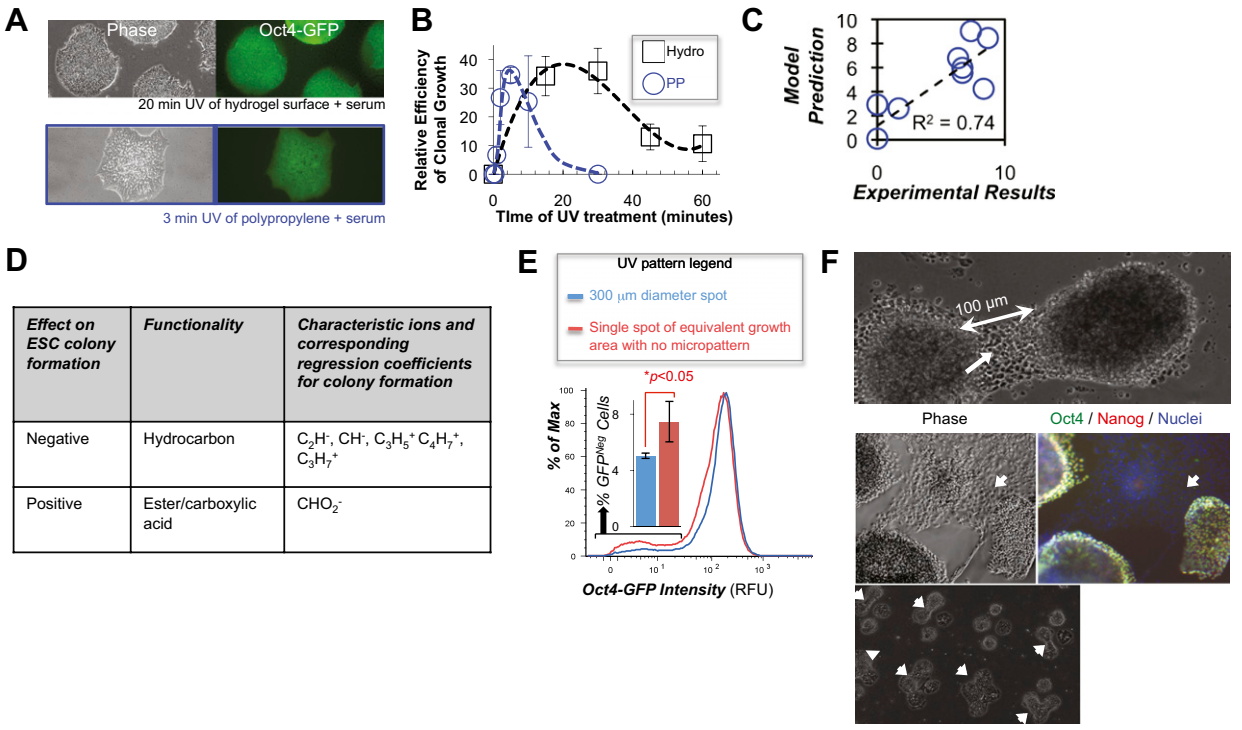

Effect on ESC colony formation	*Functionality*	*Characteristic ions and corresponding regression coefficients for colony formation*
Negative	Hydrocarbon	C_2H^-, CH^-, $C_3H_5^+$ $C_4H_7^+$, $C_3H_7^+$
Positive	Ester/carboxylic acid	CHO_2^-

Fig. S6. Surface chemical structures associated with UV treatment. (*A*) UV treatment of hydrogel-coated surfaces and polypropylene substrates supports robust colony formation. A live image of GFP fluorescence of transgenic Oct4-GFP reporter in BG01 hESCs is shown for both surfaces. The image was taken after four passages with collagenase for the hydrogel surface. (*B*) Colony formation on hydrogel-coated surface (Hydro, black squares) and polypropylene (PP, blue circles) treated with various UV doses. Colony number was assayed on day 5 after cell seeding (n = 3; error bars are 95% confidence intervals). (*C*) PLS model prediction of the number of colonies plotted against the experimental results for polypropylene. All surfaces were coated with 20% (vol/vol) FBS in DMEM-F12 base media for 15–30 min at room temperature before cell seeding. Cells were seeded in 10 μM Y-27632 ROCK inhibitor for the first 8–12 h after dissociation. (*D*) Using the PLS model of the ToF-SIMS data, surface ions with high positive or negative regression coefficients were identified as supporting or inhibiting hESC colony formation for polypropylene. (*E*) Histogram of Oct4-GFP levels of cells on patterns of 300-μm spot diameter vs. no spatial micropatterning as assayed by flow cytometry after 8 d of culture in serum-containing hESC media (15,000 cells seeded per well). The cumulative area UV-treated per well is the same for both patterns. The column graph indicates a lower percentage of differentiating Oct4-negative cells on the 300-μm diameter spots. RFU, relative fluorescent unit. (*F*) Cells can bridge UV-treated spot areas when spots are spaced ~100 μm apart (arrow indicates cell growth between spots). These cells between spots can differentiate, as indicated by down-regulation of Oct4 (green) and Nanog (red) at the arrows. In the diamond pattern, cells heterogeneously bridge the gaps as indicated by arrows when they are spaced <100 μm apart.

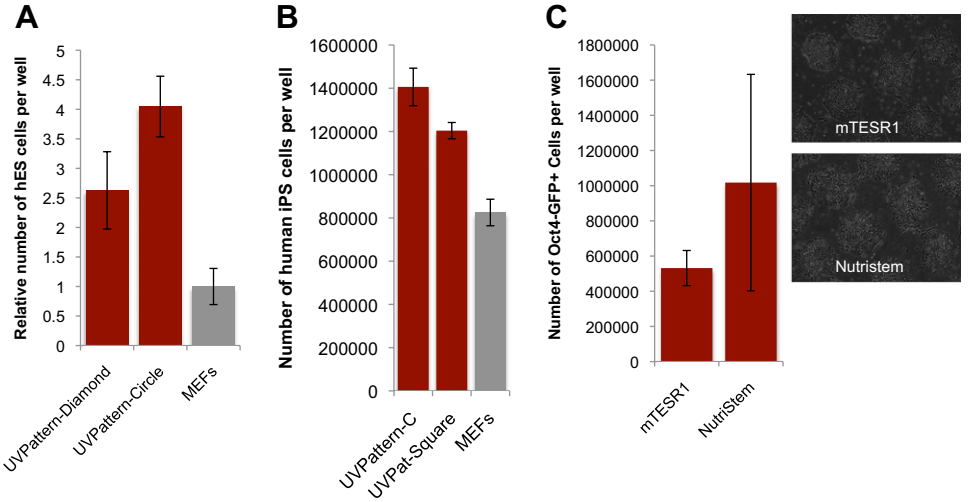

Fig. S7. Patterned substrates allow for undifferentiated cell growth in serum-free media. (*A*–*C*) Relative number of hESC colonies on UV-treated substrates with various patterns on day 7 after cell seeding. Error bars indicate 95% confidence intervals (n = 3). UVPS was coated with 20% (vol/vol) FBS in DMEM-F12 base media for 15–30 min at room temperature before cell seeding. Cells were seeded in 10 μM Y-27632 ROCK inhibitor for the first 8–12 h after dissociation. Both serum-free media, Nutristem and mTeSR1, support robust growth on UV-patterned surfaces for two passages.

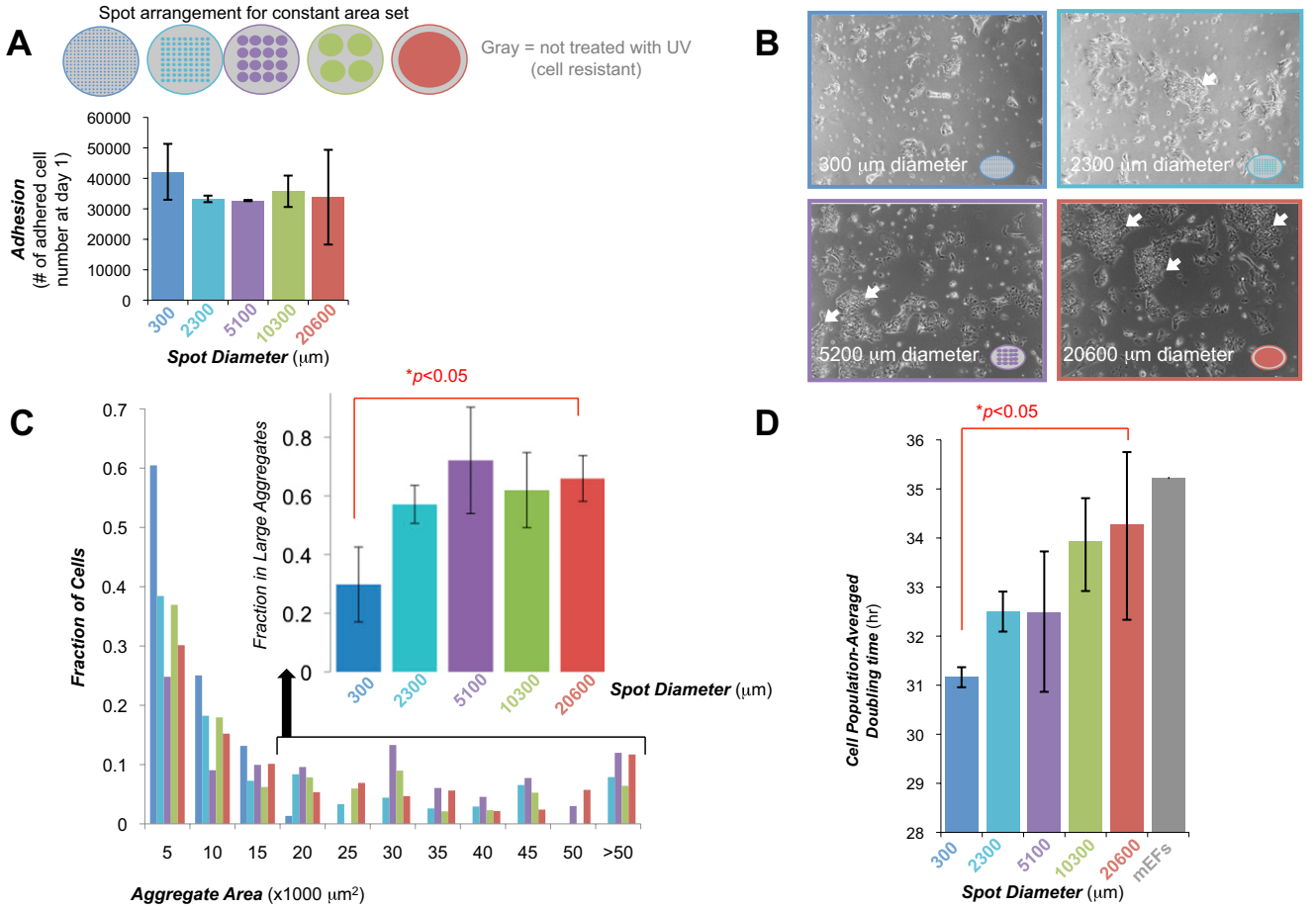

Fig. S8. Cell behavior on UV-patterned substrates. (*A*) Number of adhered cells after 24 h of culture in mTeSR1 media on the constant area patterns as described in Fig. 2*E* (40,000 cells seeded per well). No significant differences were seen across the different patterns. (*B*) Phase-contrast images of hiPSCs after 24 h of culture in mTeSR1 media on the constant area patterns as described in Fig. 2*E* (25,000 cells seeded per well). White arrows indicate large aggregates. No large aggregates were seen in the 300-μm diameter spot pattern. (*C*) Area distribution of cell aggregates seen after 24 h of culture in mTeSR1 media on the constant area patterns as described in Fig. 2*E* (12,000 cells seeded per well). (*Inset*) Column graph indicates fraction of cells contained in large (>20,000 μm^2) aggregates. As the number of spots increases, larger cell aggregates are observed. (*D*) Cell population-averaged doubling time for cells cultured on the constant area patterns for 7 d as described in Fig. 2*E* (15,000 cells seeded per well).

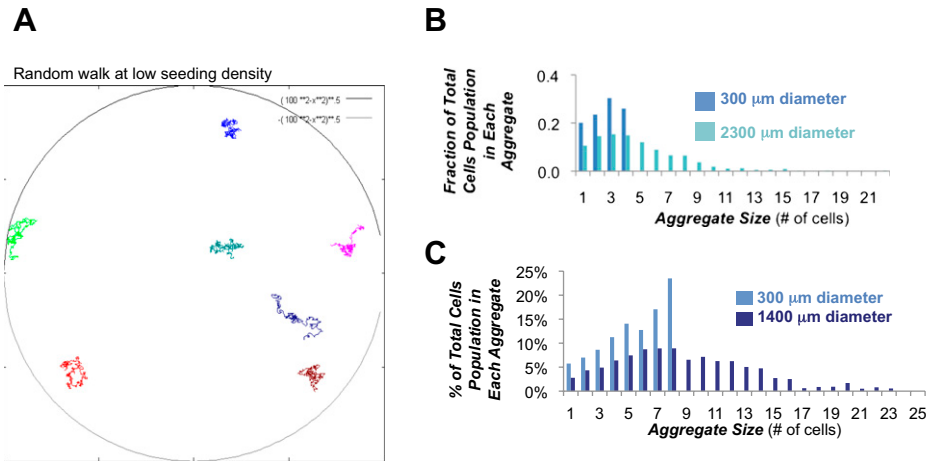

Fig. S9. Simulations of cell behavior on UV-patterned substrates. (*A*) Representative individual cell trajectories over 24 h predicted from cell migration and aggregation model on a single 600-μm spot at a low seeding density to indicate random walk. Colors indicate different cells. (*B*) Distribution of cells in each aggregate as predicted from the cell migration model for two different patterns, 300- and 2,300-μm spot diameters, at a low cell density when ROCK inhibitor is added. (*C*) Distribution of cells in each aggregate as predicted from the cell migration model for two different patterns, 300- and 1,400-μm spot diameters, when ROCK inhibitor is added at routine cell densities. In ROCK inhibitor, cells migrate faster as described by Li et al. (8). The conclusion that 300-μm diameter spots reduce large cell aggregates is consistent for both cases.

A

Plate format	Spot Diameter (μm)	Spot Spacing (μm)	# of Spots	UV treated Growth area (mm^2)	% Well Area that is UV treated
6 well	No Pattern	No Pattern	N/A	855	100.0%
6 well	20605	N/A	1	333	39.0%
6 well	10302	100	4	333	39.0%
6 well	5151	100	16	333	39.0%
6 well	2289	100	81	333	39.0%
6 well	300	100	4717	333	39.0%
6 well	300	200	3019	213	25.0%
6 well	150	100	12076	213	25.0%
6 well	150	200	6161	109	12.7%
6 well	150	400	2495	44	5.2%
6 well	300	100	4717	333	39.0%
6 well	300	200	3019	213	25.0%
6 well	300	400	1540	109	12.7%
6 well	450	100	2495	397	46.4%
6 well	450	200	1786	284	33.2%
6 well	450	400	1045	166	19.4%

B

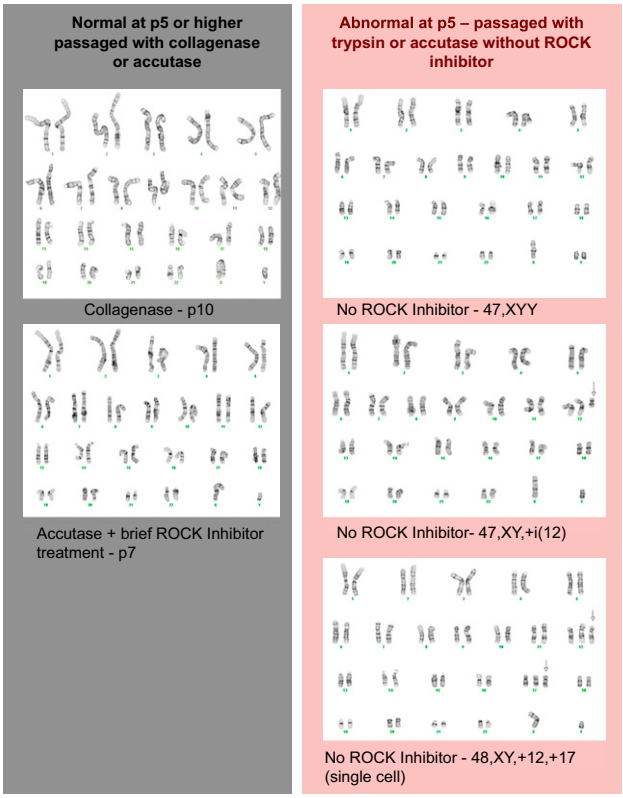

C

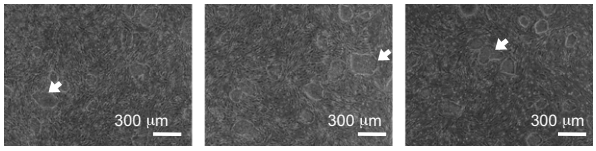

Fig. S10. Characteristics of substrates and cells on UV-patterned substrates. (*A*) Table indicating various dimensions and areas of UV-treated plates used for cell culture. (*B*) Cell cultures became abnormal within 5 passages on UV-patterned substrates when passaged under harsh conditions (with accutase or trypsin without ROCK inhibitor). In contrast, cell cultures were karyotypically normal for 7–27 passages on UV-patterned substrates when passaged with collagenase or accutase with overnight ROCK inhibitor incubation after dissociation (Fig. 6*E*). p, passage. (*C*) Representative phase-contrast images of BG01 hESCs grown on top of a mouse embryonic feeder (MEFs) layer. Arrows indicates large hESC colonies that approach a diameter of 300 μm.

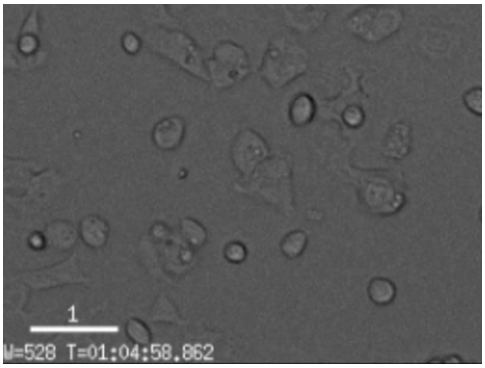

Movie S1. Bright-field video of hESCs after cell seeding on a UV-patterned substrate with a 300-μm diameter spot pattern. Images were taken every 10 min, and a counter on the bottom indicates the elapsed time since cell seeding. CO_2-independent media contained 10% (vol/vol) FBS and ROCK inhibitor. The majority of cells attach and aggregate within 3 h. Patterned substrate was coated with 20% (vol/vol) FBS for 15–30 min at room temperature before cell seeding.

Movie S1